Int J Earth Sci (Geol Rundsch) (2015) 104:75–87
DOI 10.1007/s00531-014-1064-z

ORIGINAL PAPER

Zircon U–Pb, O, and Hf isotopic constraints on Mesozoic magmatism in the Cyclades, Aegean Sea, Greece

Bin Fu · Michael Bröcker · Trevor Ireland · Peter Holden · Leslie P. J. Kinsley

Received: 18 February 2014 / Accepted: 28 July 2014 / Published online: 17 August 2014

Abstract Compared to the well-documented Cenozoic magmatic and metamorphic rocks of the Cyclades, Aegean Sea, Greece, the geodynamic context of older meta-igneous rocks occurring in the marble–schist sequences and mélanges of the Cycladic Blueschist Unit is as yet not fully understood. Here, we report O–Hf isotopic compositions of zircons ranging in age from ca. 320 Ma to ca. 80 Ma from metamorphic rocks exposed on the islands of Andros, Ios, Sifnos, and Syros with special emphasis on Triassic source rocks. Ion microprobe (SHRIMP II) single spot oxygen isotope analysis of pre-Cretaceous zircons from various felsic gneisses and meta-gabbros representing both the marble–schist sequences and the mélanges of the study area yielded a large range in $\delta^{18}O$ values, varying from 2.7 ‰ to 10.1 ‰ VSMOW, with one outlier at −0.4 ‰. Initial ε_{Hf} values (−12.5 to +15.7) suggest diverse sources for melts formed between Late Carboniferous to Late Cretaceous time that record derivation from mantle and reworked older continental crust. In particular, variable $\delta^{18}O$ and $\varepsilon_{Hf}(t)$ values for Triassic igneous zircons suggest that magmatism of this age is more likely rift- than subduction-related. The significant crustal component in 160 Ma meta-gabbros from Andros implies that some Jurassic gabbroic rocks of the Hellenides are not part of SSZ-type (supra-subduction zone) ophiolites that are common elsewhere along the margin of the Pelagonian zone.

Keywords Ion microprobe · Oxygen isotopes · Hafnium isotopes · Zircon · Attic–Cycladic Crystalline Belt

Introduction

The Cyclades in the Aegean Sea, Greece, represent a part of the Alpine-Himalayan orogenic collage and are a key area for understanding Gondwana breakup and collision between Gondwana-derived fragments and the Eurasian plate (e.g. Keay and Lister 2002). It has been generally agreed that continental rifting of northeastern Gondwana in northern Africa has been initiated during Late Carboniferous–Permian times and continued into early to mid-Triassic times, eventually leading to the creation of Neotethyan ocean basin(s) (e.g. Pe-Piper 1998 and references therein). The continental rifting resulted from extension subsequent to Hercynian subduction of the Palaeotethys ocean at an Andean-type margin (e.g. Robertson et al. 1991). However, the Triassic evolution of the western Mediterranean region is poorly understood but a significant precursor to the better documented Cenozoic history. Triassic volcanic rocks are widespread within the Hellenides and include a predominant subalkaline basalt–andesite–dacite series, and minor shoshonites and calc-alkaline rocks, alkaline basalts and mid-ocean ridge basalt (MORB)-like varieties (e.g. Pe-Piper 1998). Triassic felsic plutonic rocks are also common in different tectonic zones of the Hellenides. Such rocks intruded Permo-Carboniferous basement and record various degrees of metamorphic overprinting (e.g. Reischmann 1998; Himmerkus

Electronic supplementary material The online version of this article (doi:10.1007/s00531-014-1064-z) contains supplementary material, which is available to authorized users.

B. Fu (✉) · T. Ireland · P. Holden · L. P. J. Kinsley
Research School of Earth Sciences, The Australian National University, Canberra, ACT 0200, Australia
e-mail: bin.fu@anu.edu.au

M. Bröcker
Institut für Mineralogie, Westfälische-Wilhelms Universität Münster, Corrensstraße 24, 48149 Münster, Germany

et al. 2009; Chatzaras et al. 2013 and references therein; Fig. 1).

The geodynamic significance of the regionally widespread Triassic igneous and meta-igneous rocks has been a contentious issue and has either been related to rift-settings or to short-lived contemporaneous subduction processes, in association with the creation of one, two, or more Neotethyan oceanic basins (e.g. Koutsovitis et al. 2012; Bortolotti et al. 2013 and references therein). Several tectonic models concerning Triassic and subsequent magmatism have been proposed and are summarised in Robertson (2012) and Chatzaras et al. (2013), but as yet no generally accepted interpretation has been established.

The focus of this study is on Triassic and other Mesozoic igneous rocks and builds on previously and newly SIMS-dated (secondary ion mass spectrometry or ion microprobe) samples from the islands of Andros, Ios, Sifnos, and Syros (Bröcker and Keasling 2006; Bröcker and Pidgeon 2007). In contrast to the well-documented Tertiary granitoids (e.g. Bolhar et al. 2010, 2012) and the Cretaceous meta-igneous rocks (Fu et al. 2012) of the larger region, no study has addressed as yet the zircon O–Hf isotope characteristics of the metamorphosed pre-Cretaceous magmatic rocks. This is surprising because O–Hf isotope data have a considerable potential to unravel petrogenetic processes. For example, Hf isotopic ratios of zircons in crustal rocks can be used to constrain crustal residence ages, or the average time since the parental magmas were extracted, e.g. from depleted mantle, whereas the oxygen isotopic fractionation can give an indication as to the nature of processing of material. Combined zircon O–Hf isotopic systematics can distinguish between juvenile components and parental magmas derived from reworking of pre-existing crustal material and thus can help determine the magma sources (e.g. DePaolo 1981; Hawkesworth and Kemmp 2006). Such data are important because it can contribute to a better understanding of the geodynamic processes operating through geological time in the Aegean region.

Geological background and sample description

In the context of the present study, three tectonic zones of the Hellenides are of special importance: the Vardar Zone, the Pelagonian Zone, and the Attic–Cycladic Crystalline Belt. The study area is part of the Attic–Cycladic Crystalline Belt (Fig. 1) which is built from two major tectonic units recording different pressure–temperature–deformation–time (*P–T–D*–t) histories (e.g. Dürr et al. 1978; Okrusch and Bröcker 1990; Ring et al. 2010). The structurally higher unit is only preserved in relatively small occurrences and includes a heterogeneous sequence of unmetamorphosed Permian to Mesozoic sediments, ophiolites, and greenschist facies rocks with Cretaceous to Tertiary metamorphic ages (e.g. Bröcker and Franz 1998, 2006), as well as Late Cretaceous granitoids and medium-pressure/high-temperature metamorphic rocks (e.g. Patzak et al. 1994 and references therein). The structurally lower unit (=Cycladic Blueschist Unit) consists of a pre-Alpine crystalline basement and a stack of tectonic subunits that is composed of metamorphosed volcano-sedimentary rocks and mélanges. The Cycladic Blueschist Unit has experienced Tertiary eclogite- to epidote-blueschist facies metamorphism and various degrees of greenschist- to upper-amphibolite facies overprinting (e.g. Okrusch and Bröcker 1990; Ring et al. 2010).

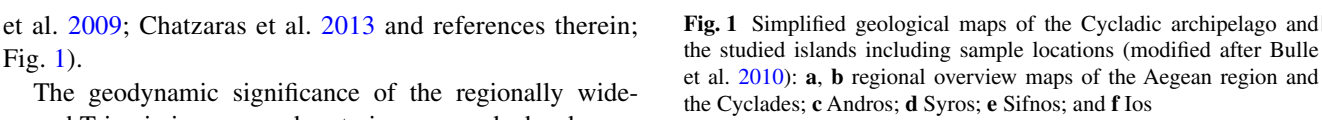

Fig. 1 Simplified geological maps of the Cycladic archipelago and the studied islands including sample locations (modified after Bulle et al. 2010): **a**, **b** regional overview maps of the Aegean region and the Cyclades; **c** Andros; **d** Syros; **e** Sifnos; and **f** Ios

Details of the geology of the Cyclades have been described in numerous contributions and the geological and tectonometamorphic history of individual islands is well documented. Islands with many features relevant for the present study include: Syros (Dixon and Ridley 1987; Trotet et al. 2001a, b; Schumacher et al. 2008; Bulle et al. 2010; Keiter et al. 2011), Sifnos (Schliestedt 1986; Schliestedt and Matthews 1987; Avigad et al. 1992; Avigad 1993; Trotet et al. 2001a, b; Schmädicke and Will 2003; Groppo et al. 2009), Andros (Papanikolaou 1978; Mukhin 1996; Bröcker and Franz 2006; Huyskens and Bröcker 2014), and Ios (Henjes-Kunst and Kreuzer 1982; van der Maar and Jansen 1983; Baldwin and Lister 1998; Forster and Lister 1999; Huet et al. 2009; Thomson et al. 2009).

The analysed zircon populations are mostly from previously dated samples of the Cycladic Blueschist Unit that yielded Cretaceous, Jurassic, or Triassic protolith ages (Bröcker and Keasling 2006; Bröcker and Pidgeon 2007) and include rocks representing both the marble–schist sequences (Andros, Sifnos, Ios) and blocks from high-pressure/low-temperature mélanges (Syros, Andros). Cretaceous and Jurassic ages have only been documented for mélange blocks, whereas Triassic ages were reported for tectonic slabs in mélanges and for layers within schist successions. Sample-specific information such as rock type, location details, and U–Pb zircon ages is summarised in Table 1. For details of the local geology and mineral assemblages see Bröcker and Keasling (2006), Bröcker and Pidgeon (2007) and Bulle et al. (2010). Most zircon ages for the ten meta-igneous samples are interpreted to reflect the timing of magmatism at ca. 240 Ma (7 samples), ca. 160 Ma (2), and ca. 80 Ma (1); only two of them (samples 5008 and 4036) contain inherited zircon cores (ca. 1,414–273 Ma) (Bröcker and Keasling 2006; Bröcker and Pidgeon 2007).

This sample suite is complemented by the gneissic rocks 5039 and 5041 (Electronic supplementary materials or

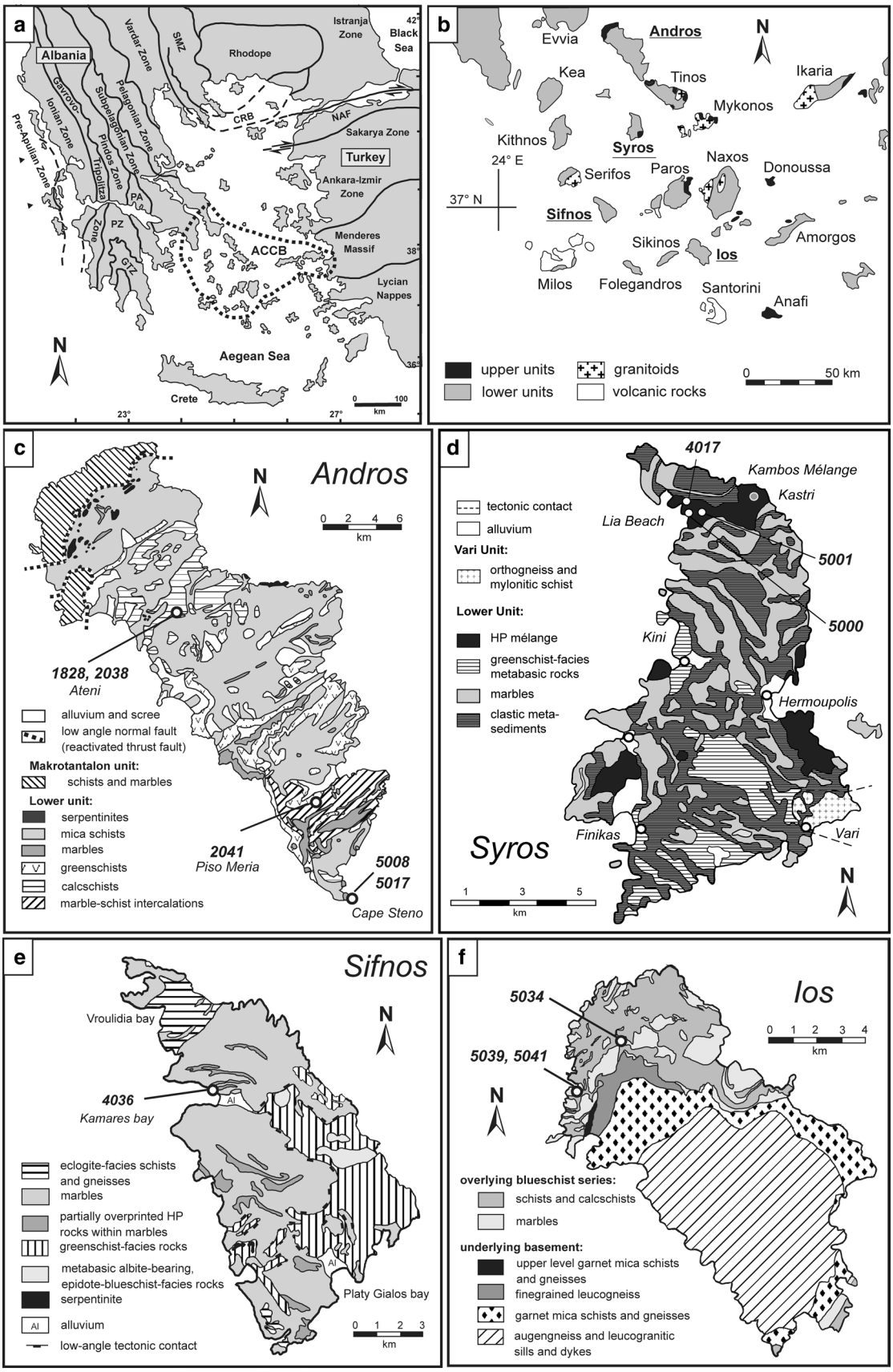
a
Albania
Gavrovo
Ionian Zone
Pre-Apulian Zone
Vardar Zone
SMZ
Rhodope
Istranja Zone
Black Sea
Pelagonian Zone
Subpelagonian Zone
Pindos Zone
Tripolitza
PA
PZ
Zone
CRB
NAF
Sakarya Zone
Turkey
Ankara-Izmir Zone
ACCB
Menderes Massif
OTZ
Lycian Nappes
Aegean Sea
Crete
N
23°
27°
38°
36°
0 100 km
b
Evvia
Andros
Kea
Tinos
Ikaria
Mykonos
Kithnos
Syros
Serifos
Paros
Naxos
Donoussa
24° E
37° N
Sifnos
Sikinos
Ios
Amorgos
Milos
Folegandros
Santorini
Anafi
upper units
lower units
granitoids
volcanic rocks
0 50 km
c
Andros
N
0 2 4 6 km
1828, 2038
Ateni
alluvium and scree
low angle normal fault
(reactivated thrust fault)
Makrotantalon unit:
schists and marbles
Lower unit:
serpentinites
mica schists
marbles
greenschists
calcschists
marble-schist intercalations
2041
Piso Meria
5008
5017
Cape Steno
d
4017
Kambos Mélange
Kastri
Lia Beach
5001
5000
Kini
Hermoupolis
Finikas
Vari
Syros
N
1 3 5 km
tectonic contact
alluvium
Vari Unit:
orthogneiss and
mylonitic schist
Lower Unit:
HP mélange
greenschist-facies
metabasic rocks
marbles
clastic meta-
sediments
e
Sifnos
N
Vroulidia bay
4036
Kamares bay
Al
Platy Gialos bay
0 1 2 3 km
eclogite-facies schists
and gneisses
marbles
partially overprinted HP
rocks within marbles
greenschist-facies rocks
metabasic albite-bearing,
epidote-blueschist-facies rocks
serpentinite
alluvium
low-angle tectonic contact
f
Ios
5034
5039, 5041
N
0 1 2 3 4 km
overlying blueschist series:
schists and calcschists
marbles
underlying basement:
upper level garnet mica schists
and gneisses
finegrained leucogneiss
garnet mica schists and gneisses
augengneiss and leucogranitic
sills and dykes

Table 1 Samples from Andros, Ios, Sifnos, and Syros, Greece

Island	Sample no. (Mount no.)	Lithology	Locality (Latitude, Longitude)	Age[a] (2σ; Ma)
Andros	5017 (MB6)	Meta-gabbro in mélange	Cape Steno (N37°41.055′, E24°57.754′)	156.2 ± 2.3
	5008 (MB7)	Felsic gneiss in mélange	Cape Steno (N37°41.107′, E24°57.544′)	Mainly 160.0 ± 2.0
	2041 (MB2)	Felsic gneiss (status unclear: tectonic block or boudinaged layer)	Piso Meria (N37°44.905′, E24°55.824′)	240.0 ± 1.4
	1828 (MB5)	Felsic gneiss (status unclear: tectonic block or boudinaged layer)	Ateni (N37°52.518′, E24°48.636′)	241.3 ± 1.9
	2038 (MB5)	Felsic gneiss (status unclear: tectonic block or boudinaged layer)	Ateni (N37°52.733′, E24°48.736′)	249.4 ± 2.0
Sifnos	4036 (MB2)	Meta-tuffaceous gneiss (layer in schist sequence)	Kamares (N36°59.773′, E24°40.207′)	Mainly ~240
Ios	5034 (MB7)	Felsic gneiss (layer in schist sequence)	Ios (N36°45.687′, E25°17.140′)	237.1 ± 4.4
	5039 (BF032 and MB7)	Meta-tuffaceous gneiss (layer in schist sequence)	Ios (N36°44.658′, E25°15.792′)	Mainly 243.3 ± 3.3
	5041 (BF032 and MB6)	Meta-tuffaceous gneiss (layer in schist sequence)	Ios (N36°44.658′, E25°15.792′)	Mostly 318.6 ± 2.7
Syros	4017 (MB6)	Meta-plagiogranitic domain in a meta-gabbro mélange block	Kampos mélange (N37°29.704′, E24°54.005′)	76.6 ± 1.3
	5001 (MB2)	Felsic gneiss (tectonic slab in mélange)	Kampos mélange (N37°29.466′, E24°54.296′)	240.1 ± 4.1
	5000 (MB5)	Felsic gneiss (tectonic slab in mélange)	Kampos mélange (N37°29.444′, E24°54.089′)	245.3 ± 4.9

[a] Age data sources: samples (5039 and 5041), this study; the others, Bröcker and Keasling (2006) and Bröcker and Pidgeon (2007)

ESM S1) from Ios, which occur as coherent layers within schist sequences. Both rocks mainly consist of quartz, plagioclase, epidote/clinozoisite, chlorite, white mica, and sphene. Relict blue amphibole is preserved in sample 5039. It is often very difficult to decipher the parent rock type of meta-felsic rocks and this is also true for these quartz and feldspar-rich samples. Original textural features of the protoliths have been completely erased by metamorphic and deformational overprinting. Bulk geochemical data are not available and likely would not be useful for identification of the protolith in any case.

Analytical methods

The available zircon mounts (MB2, MB5, MB6 and MB7: Bröcker and Keasling 2006; Bröcker and Pidgeon 2007) from SHRIMP (Sensitive High-Resolution Ion Micro-Probe) U–Pb analysis contained relatively small pieces of standard zircon CZ3 that were supplemented by one or two large grains of face-mounted standard zircon Plešovice for SHRIMP $^{18}O/^{16}O$ analysis. The pits from previous ion-probe age dating were polished out. Mount BF032 was newly prepared for samples 5039 and 5041 from Ios. For this purpose, hand-picked zircons and grains of the standards (Plešovice and Temora-2) were cast in epoxy, ground, and polished to expose the midsection of the grains, and cathodoluminescence (CL) imaging was conducted using a JEOL JSM-6610A Analytical SEM (scanning electron microscope) in Research School of Earth Sciences (RSES), The Australian National University (ANU), Canberra, equipped with a Robinson CL detector. Representative SEM-CL images of zircons from some of the studied samples are shown in Fig. 2.

The instruments employed include SHRIMP-RG (Reverse Geometry) for U–Pb geochronology, SHRIMP II and SHRIMP SI (Stable Isotope) for O isotopes, and laser ablation—multi-collector—inductively coupled plasma mass spectrometry (LA–MC-ICP-MS) for Hf isotopes, all at RSES, ANU. The analytical procedures and data processing are described in detail in ESM S1 and summarised below. U–Th–Pb isotopic analyses of zircons were carried out on the SHRIMP-RG ion microprobe. Analytical procedures are similar to those described in Williams (1998 and references therein) and Ireland and Williams (2003). Data were reduced using the SQUID Excel Macro of Ludwig (2001a) and the ISOPLOT/EX Excel Macro of Ludwig (2001b). Oxygen isotope ratios ($^{18}O/^{16}O$) of zircons were determined using SHRIMP II and SHRIMP SI ion microprobes. Analytical conditions were similar to those outlined in detail by Ickert et al. (2008). In situ Lu–Hf isotope analyses for zircons were carried out using the 193 nm excimer laser-based HELEX ablation system coupled to a Neptune MC-ICP-MS described in Eggins et al. (2005). Data were reduced offline using the software package Iolite (Paton et al. 2011). The microanalytical results are tabulated in ESM S2 to S4.

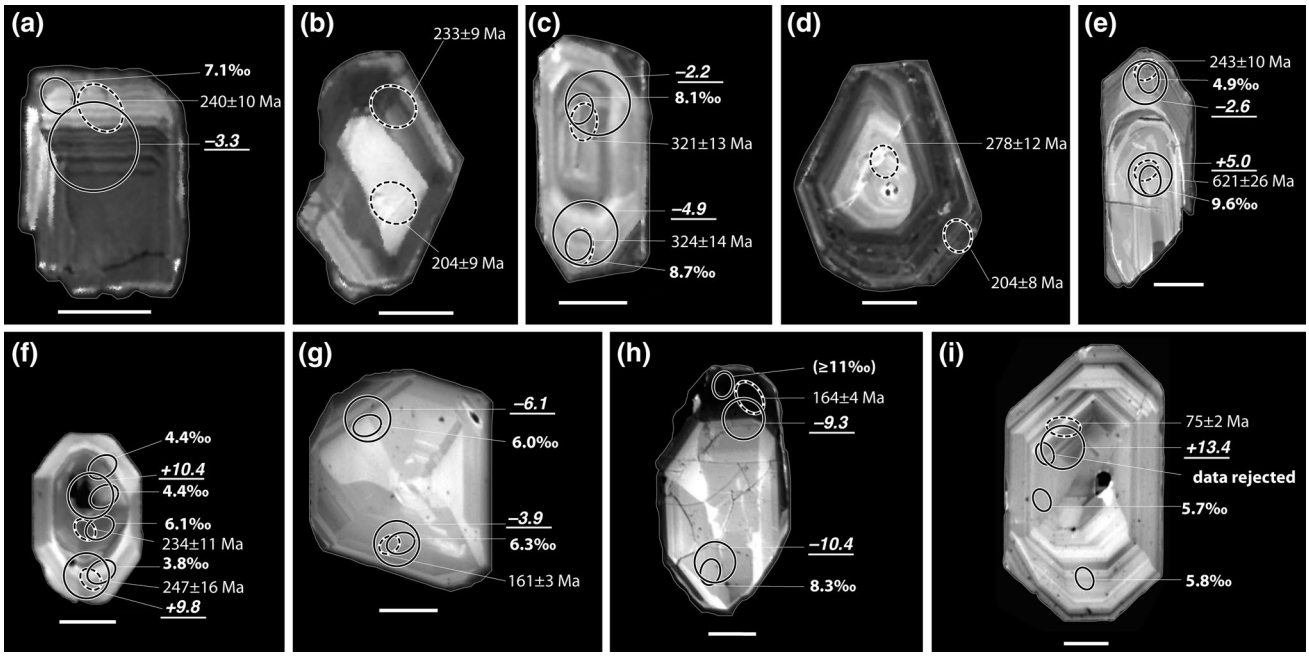

Fig. 2 Cathodoluminescence images and U–Pb ages and O–Hf isotopic ratios for representative zircon grains from meta-igneous rocks from Andros, Ios, Sifnos, and Syros, Greece: **a** grain no. 5 and **b** grain no. 1, gneissic rock sample 5039; **c** grain no. 26 and **d** grain no. 2, gneissic sample 5041, from Ios; **e** grain no. 19, meta-tuffaceous gneiss sample 4036, from Sifnos; **f** grain no. 21, felsic gneiss sample 2041; **g** grain no. 30, felsic gneiss sample 5008; **h** grain no. 11, meta-gabbro sample 5017, from Andros; and **i** grain no. 35, meta-plagiogranitic sample 4017, from Syros. *Numbers* represent SIMS U–Pb ages (±2σ; *dash ellipse*) and $\delta^{18}O$ values (also *ellipse*) and LA-ICP-MS initial epsilon Hf or $\varepsilon_{Hf}(t)$ values (*italic*, *underlined*; *circle*). Data sources: ages for **e** to **i**, from Bröcker and Keasling (2006) and Bröcker and Pidgeon (2007); others, this study. *Scale bars* 50 μm

Results

Zircon U–Pb geochronology

In addition to the previously dated samples in Table 1, U–Pb geochronology was carried out on samples 5039 and 5041 from Ios, which most likely represent meta-tuffaceous protoliths. Zircon of both samples is mostly characterised by short, sharp, pyramidal terminations in morphology and oscillatory zonation as revealed by CL imaging (Fig. 2a–d). Rounded surfaces typical for detrital zircons are not seen; distinct core–rim structures are rarely developed. A total of 33 SIMS spot analyses of 32 grains from sample 5039 yielded a wide range in ages, from 567 to 204 Ma (Fig. 3a). The majority of grains contribute to a single peak in the age distribution at around 240 Ma (inset of Fig. 3a). The weighted mean $^{206}Pb/^{238}U$ age calculated from 258 to 204 Ma data points shows excess scatter with main contribution from the two youngest grains. Eliminating these two analyses gives a weighted mean age of 243.3 ± 3.3 Ma (95 % confidence level (c.l.), MSWD = 2.4, n = 25). The zircons in this group have U and Th concentrations of 106–1,017 and 31–861 ppm, respectively, and Th/U ranges between 0.29 and 0.97. Five older zircons (331–293 Ma) and two younger zircons or domains (weakly zoned rim: 210 ± 9 Ma, 2σ; bright, homogeneous core: 204 ± 9 Ma) have Th and U concentrations of 169–578 and 50–340 ppm, respectively, and Th/U ratios (0.18–0.61). Th and U concentrations in the oldest zircon (567 Ma) are 16 and 187 ppm, respectively, with Th/U ratio of 0.1, possibly of metamorphic origin.

Fifty analyses of 39 zircon grains from sample 5041 yielded ages between 620 and 204 Ma although most zircons are around 320 Ma. The weighted mean $^{206}Pb/^{238}U$ age calculated by trimming tails for a major group of age varying from 334 to 299 Ma, as seen in a probability density diagram (inset of Fig. 3b), is 318.6 ± 2.7 Ma (95 % c.l., MSWD = 1.5, n = 39). The zircons in this group have U and Th concentrations of 72–2,029 and 22–344 ppm; Th/U ratios vary between 0.12 and 0.59. A second age group of zircons or distinct domains within individual grains (286–268 Ma) are characterised by a weighted mean $^{206}Pb/^{238}U$ age = 279 ± 12 Ma (95 % c.l., MSWD = 0.19, n = 7), U = 155–2,075 ppm, Th = 55–275 ppm, Th/U = 0.11–0.61. U and Th concentrations in two older zircons or domains (620, 517 Ma) are: 25 and 166 ppm, 33 and 45 ppm, respectively, and their Th/U ratios are 1.4 and 0.3. Two zircons have much younger zoned rims, 210 ± 8 Ma (2σ) and 204 ± 8 Ma, similar to the above sample, than the bright cores. Their Th/U ratios are identical at 0.2, with

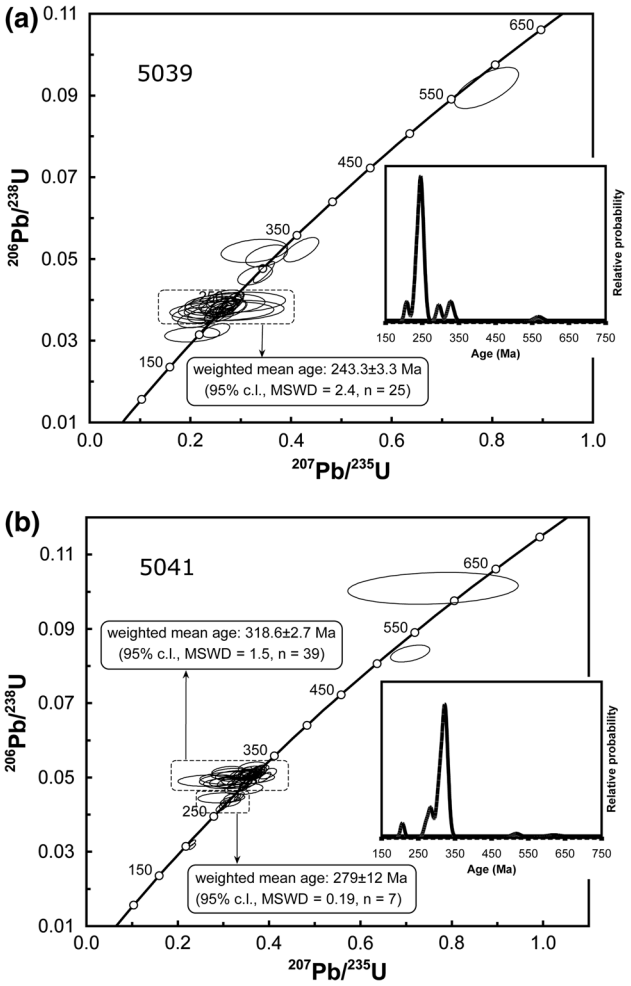

Fig. 3 Concordia diagrams for zircons of gneiss samples 5039 and 5041 from Ios. *Insets* are probability density diagrams. *Data-point error ellipses* denote 2σ errors

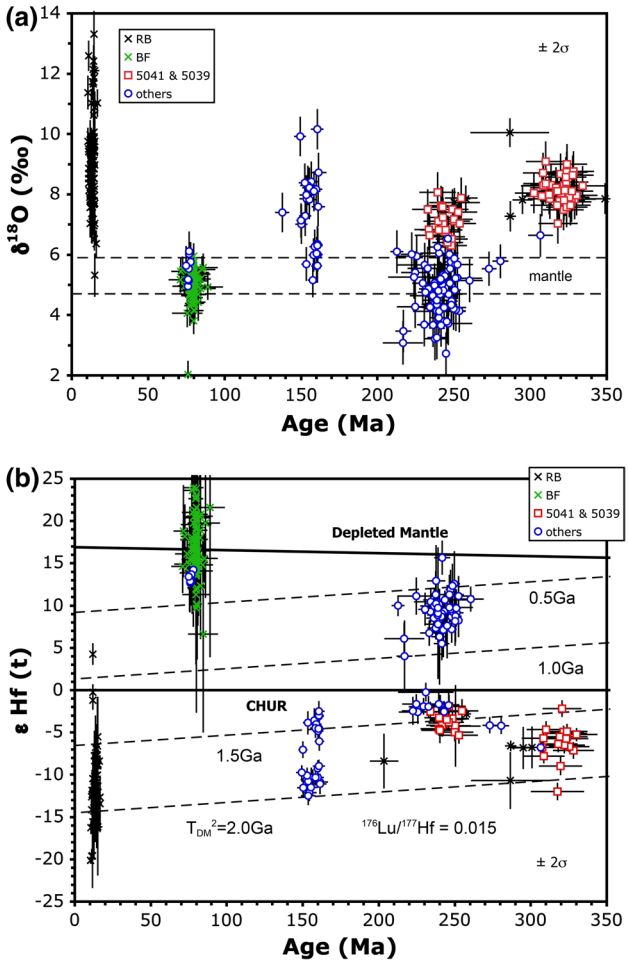

Fig. 4 Ages plotted against **a** ion microprobe $\delta^{18}O$ values of zircons from meta-igneous rocks from Andros, Ios, Sifnos, and Syros, Greece; and **b** LA-ICP-MS initial epsilon Hf values. *Dashed horizontal lines* in **a** indicate the compositional range of igneous zircons from the mantle and in equilibrium with primitive magmatic compositions ($\delta^{18}O = 5.3 \pm 0.6$ ‰, 2σ; Valley et al. 2005). Published data for zircons from Cretaceous and Cenozoic igneous or meta-igneous rocks in the region are also plotted for comparison: RB, Bolhar et al. (2010, 2012); BF, Fu et al. (2010, 2012)

U = 2,275 ppm and 1,705 ppm and Th = 486 ppm and 346 ppm, respectively.

Oxygen isotopic compositions

The $\delta^{18}O$ and $\varepsilon_{Hf}(t)$ values for all zircon spot analyses plotted against ages are shown in Fig. 4 and averages for individual samples are summarised in Table 2. The zircon O–Hf isotopic data, available for many of the dated zircons with concordant age, are presented in Figs. 2, 4, and 5.

The $\delta^{18}O$ values from the peak 320-Myr-old zircons of sample 5041 (Ios) range from 7.0 to 9.0 ‰. The ca. 240 Ma zircons from sample 5039 indicate comparably high $\delta^{18}O$ values, ranging from 6.2 to 8.2 %. It is noted that $\delta^{18}O$ values for two Carboniferous zircon grains of this sample (7.4 and 7.8 ‰) fall within the range for sample 5041. The Triassic zircon populations of 6 meta-igneous samples from Andros (2041, 1828 and 2038) Ios (5034), and Syros (5001 and 5000) are characterised by $\delta^{18}O$ values varying from 2.7 to 6.0 %; $\delta^{18}O$ (zircon) for sample 4036 from Sifnos ranges between 4.1 and 6.5 ‰, excluding one outlier of −0.4 ‰ and inherited cores. $\delta^{18}O$ for Jurassic zircons from two meta-igneous samples range from 5.2 to 7.2 ‰ (sample 5008) and from 6.9 ‰ to 10.1 ‰ (sample 5017), respectively. Five inherited zircon grains or zircon cores of Proterozoic to Permian age from samples 5008 and 4036 record a wide range in $\delta^{18}O$ (5.6–9.6 ‰).

Cretaceous zircons from meta-plagiogranite 4017 yielded $\delta^{18}O$ values of 4.9 to 6.0 ‰. These largely overlap with the 'mantle-like' values ($\delta^{18}O$: 4.7–5.5 ‰) reported for 80-Myr-old zircons of other mélange blocks and matrix rocks from Tinos and Syros (Fu et al. 2012).

Table 2 Oxygen and hafnium isotope compositions of zircon in selected samples from Andros, Ios, Sifnos, and Syros, Greece, analysed by SHRIMP II and calibrated against Plešovice (8.19 ± 0.08 ‰; J.W. Valley, unpublished data in Fu et al. 2012)

Island	Sample no.	Lithology	Av. $\delta^{18}O \pm 2\sigma$[a] (‰; # of analyses)	$\varepsilon_{Hf}(t)$[a]
Andros	5017	Meta-gabbro in mélange	8.1 ± 1.7 (16)	–10.6 ± 1.8 (16) (t = 160 Ma)
	5008	Felsic gneiss in mélange	6.1 ± 1.0 (14)	–3.8 ± 1.5 (12) (t = 160 Ma)
	2041	Felsic gneiss (status unclear: tectonic block or boudinaged layer)	4.7 ± 1.1 (27)	10.1 ± 2.2 (13) (t = 240 Ma)
	1828	Felsic gneiss (status unclear: tectonic block or boudinaged layer)	5.0 ± 1.4 (10)	8.9 ± 3.9 (10) (t = 240 Ma)
	2038	Felsic gneiss (status unclear: tectonic block or boudinaged layer)	4.9 ± 1.5 (12)	9.6 ± 3.6 (10) (t = 240 Ma)
Sifnos	4036	Meta-tuffaceous gneiss (layer in schist sequence)	5.4 ± 1.2 (23)[b]	–1.7 ± 1.4 (10) (t = 240 Ma)
Ios	5034	Felsic gneiss (layer in schist sequence)	5.1 ± 0.5 (16)	8.1 ± 2.0 (15) (t = 240 Ma)
	5039	Meta-tuffaceous gneiss (layer in schist sequence)	7.0 ± 1.0 (31)	–3.9 ± 2.0 (15) (t = 240 Ma)
	5041	Meta-tuffaceous gneiss (layer in schist sequence)	8.1 ± 0.9 (43)	–6.3 ± 4.1 (17) (t = 240 Ma)
Syros	4017	Meta-plagiogranitic domain in a meta-gabbro mélange block	5.5 ± 0.8 (10)	13.3 ± 1.0 (8) (t = 80 Ma)
	5001	Felsic gneiss (tectonic slab in mélange)	4.0 ± 1.4 (21)	9.9 ± 2.2 (7) (t = 240 Ma)
	5000	Felsic gneiss (tectonic slab in mélange)	3.8 ± 1.9 (7)	11.6 ± 5.2 (6) (t = 240 Ma)

[a] $\delta^{18}O$ and $\varepsilon_{Hf}(t)$ for inherited zircons are excluded from calculation

[b] An outlier is omitted from calculation

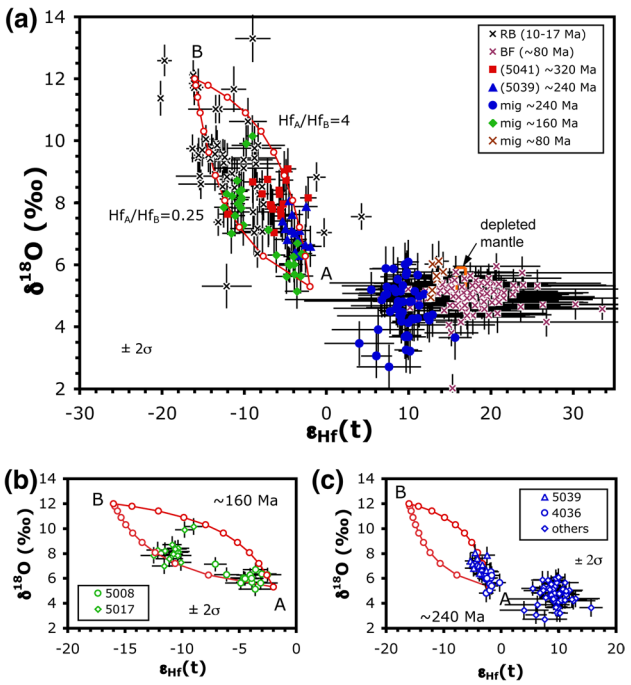

Fig. 5 $\delta^{18}O$ versus $\varepsilon_{Hf}(t)$ values for zircons from meta-igneous (mig) rocks from Andros, Ios, Sifnos, and Syros, Greece: **a** all ages (for data sources and abbreviations, see Fig. 4); **b** Jurassic; and **c** Triassic (others: samples 1828, 2038, 2041, 5000, 5001 and 5034). Data for inherited zircon grains are excluded. See text for endmembers A and B and explanations

Hafnium isotopic compositions

Fifteen out of 17 analyses (by LA–MC-ICP-MS) of zircons from sample 5041 (Ios) yielded $^{176}Hf/^{177}Hf$ ratios of 0.282328–0.282458, corresponding to $\varepsilon_{Hf}(t)$ values of −9.0 to −4.7 (Fig. 4b). Measured $^{176}Lu/^{177}Hf$ and $^{176}Hf/^{177}Hf$ ratios of ca. 240 Ma zircons from sample 5039 range from 0.000631 to 0.002460 and from 0.282439 to 0.282574, respectively, corresponding to $\varepsilon_{Hf}(t)$ values of −5.3 to −1.9 (Fig. 4b). One older zircon grain has an $\varepsilon_{Hf}(t$ = 322 Ma) value as low as −5.0, within the range given for the ca. 320 Ma zircons from sample 5041.

The Triassic zircons from meta-igneous samples have $\varepsilon_{Hf}(t)$ values of −2.6 to −0.3 for one sample (4036) and +5.5 to +15.7 for the other 6 samples. $\varepsilon_{Hf}(t)$ for Jurassic zircons from two meta-igneous samples range from −4.9 to −2.5 (sample 5008) and from −12.5 to −9.0 (sample 5017). Seven inherited zircon grains or zircon cores (ca. 273–1,414 Ma) of samples 4036 and 5008 indicate a wide range in $\varepsilon_{Hf}(t)$ (−19.0 to +5.0).

The $\varepsilon_{Hf}(t)$ values for Cretaceous zircons from the meta-plagiogranite 4017 vary from +12.7 to +14.2. The results are close to that reported for other contemporaneous mélange blocks and matrix rocks in the same region (Fu et al. 2012), interpreted to be derived from depleted MORB mantle or similar sources.

Discussion

There are four major zircon U–Pb age groups in the investigated samples: ca. 320 Ma, ca. 240 Ma, ca. 160 Ma, and ca. 80 Ma (Table 1). The group of Cretaceous zircons can clearly be distinguished by their contrasting O–Hf isotopic signatures from the Late Carboniferous, Late Jurassic, and most of the Triassic zircons (Fu et al. 2012; this study).

Zircon isotope characteristics through time

The morphological representation of zircons from the two Ios samples (5039, 5041), that is, sharp, pyramidal terminations with rarely developed core–rim structures, and their U–Pb ages can best be reconciled by assuming a largely igneous protolith (i.e. tuffaceous rock), derived from a proximal magmatic source, with a distinct detrital component. Hafnium depleted mantle model ages (T_{DM}) for zircon of the main Hercynian age group from sample 5041 (Ios) range from 1.4 to 1.0 Ga (ESM S4), consistent with Nd-depleted mantle model ages of ca. 1.3–1.1 Ga for the Thessaly Hercynian plutons on mainland Greece (e.g. Pe-Piper 1998). Together with the presence of inherited zircons of Late Precambrian age in two Triassic (meta-) igneous rocks (samples 5008 and 4036; Bröcker and Pidgeon 2007), this is characteristic of the West African craton (e.g. Keay and Lister 2002; Meinhold et al. 2008). Combined high $\delta^{18}O$ values and negative $\varepsilon_{Hf}(t)$ values indicate that the related parental igneous rocks record reworking of continental crust in the context of Variscan (or Hercynian) orogenic processes, as also documented in the Late Carboniferous intrusions exposed in the External Hellenides on the island of Kithira (Xypolias et al. 2006). Magmatism at such a large scale was caused by Late Paleozoic continental collision between Gondwana and Laurasia to form the supercontinent Pangaea (e.g. von Raumer 1998; Murphy et al. 2009).

The studied sample suite includes 8 (out of 12) meta-igneous rocks with Triassic protolith ages. Prominent Triassic age clusters are also a striking feature of detrital zircon populations from the Cyclades (Keay 1998; Löwen et al. 2014; Bröcker et al. 2014a) further emphasizing the importance of magmatic activity at that time for the wider region. Petrogenetic processes involved in forming igneous rocks, such as assimilation and fractional crystallization, can be examined through a plot of $\delta^{18}O$ versus $\varepsilon_{Hf}(t)$ (DePaolo 1981; Hawkesworth and Kemmp 2006). Triassic igneous zircons yielded both positive and negative $\varepsilon_{Hf}(t)$ values and variable $\delta^{18}O$ values (Figs. 4, 5). The slightly lower-than-depleted mantle $\varepsilon_{Hf}(t)$ values for zircons of some Triassic samples (2041, 1828, and 2038 from Andros, 5034 from Ios, 5001 and 5000 from Syros) may be explained by contributions of juvenile components such as recycled lower crust of an ancient island arc and/or a slab component (oceanic crust or sediments) in the mantle wedge (e.g. Nowell et al. 1998; Woodhead et al. 2001). In some modern arcs, a deviation from depleted mantle in $\varepsilon_{Hf}(t)$ as well as $\delta^{18}O$ can be related to source contamination processes in the mantle induced by subducted oceanic crust and overlying terrigenous sediments, distinguishable from assimilation of continent crust into arc magmas (e.g. Roberts et al. 2013). A melt source close to MORB-type composition is inferred for island arc magmatism, whereas subduction-related magmatism is characterised by lower $\varepsilon_{Hf}(t)$ values than MORB. Here, the mantle-like oxygen isotopic signature for the above described Triassic igneous zircon samples suggests that the high $\varepsilon_{Hf}(t)$ values are related to a less depleted melt source than MORB-type mantle, e.g. enriched mantle (EM) and high-μ (HIMU) mantle reservoirs (Pfänder et al. 2007; Geldmacher et al. 2011), with little involvement of older crustal material. The EM components may have higher $\delta^{18}O$ values than the HIMU mantle components, due to contamination of subducted sediments with the basaltic portion in recycled oceanic crust, that is, MORB-type basalts (Eiler 2001).

In contrast, the negative $\varepsilon_{Hf}(t)$ values for the zircon sample 4036 from Sifnos can be interpreted to reflect different magma sources such as existing continental crust. Inherited zircons in Triassic meta-igneous rocks indicate a composite nature of the zircon populations recording different phases of melting and crystallisation since the Precambrian. These inherited zircons are attributed to either a Precambrian continental crust or clastic sediments subducted below an ancient volcanic arc. The O–Hf isotopic ratios suggest variations in melt composition somewhere between a crustal end member and a depleted (MORB-type) mantle source and this favours a continental margin setting during Triassic time. It is noted that both positive and negative $\varepsilon_{Hf}(t)$ values reported for zircons from the Trans-Himalayan batholiths (i.e. Kohistan–Ladakh–Gangdese granites) on the southern margin of the Lhasa Terrane, southern Tibet, are attributed to island arc sources (Ji et al. 2009 and references therein). Therefore, we propose that those Triassic felsic rocks from the Cyclades characterised by high and positive $\varepsilon_{Hf}(t)$ values and mantle-like (and/or slightly lower than mantle) $\delta^{18}O$ values formed from metasomatised mantle (cf. Perkins et al. 2006), whereas those Triassic felsic rocks characterised by negative $\varepsilon_{Hf}(t)$ values and high $\delta^{18}O$ values formed either by magma mixing or from lower continental crust.

Partial melting of subducted oceanic crust, which would result in the formation of adakite, is unlikely because there are no Triassic adakites or adakitic rocks reported in the region (e.g. Pe-Piper and Piper 2002). It is noted that, in some cases, upper oceanic lithosphere may have $\delta^{18}O$ values of >7 ‰ (Bindeman et al. 2005; Martin et al. 2011), distinct from typical peridotitic mantle (and melts thereof) that exhibits a narrow range in $\delta^{18}O$ values of 5.5 ± 0.4 ‰ (Eiler 2001). The estimated Hf two-stage model ages (T^2_{DM}) are mostly Mesoproterozoic, for zircons from two samples (5039 and 4036), or Neoproterozoic, for other Triassic samples (ESM S4). This further suggests that Triassic magmas in the region may be derived from different source regions.

It is intriguing that Jurassic zircons from the meta-gabbro 5017 have higher $\delta^{18}O$ values but lower $\varepsilon_{Hf}(t)$ values

than those determined for felsic gneiss 5008 from the same high-pressure mélange on Andros (Figs. 4, 5). These rocks are believed to represent SSZ-type (supra-subduction zone) rather than MOR-type (mid-ocean ridge) ophiolites, linked to the Vardar Ocean or a different coeval oceanic basin (Bröcker and Pidgeon 2007). The Jurassic ophiolites formed either within the Pindos (-Mirdita) oceanic basin between the Apulian (or Adria) and Pelagonian continental unit or within the Vardar ocean further east (see review in Robertson 2012). However, the high $\delta^{18}O$ values of the meta-gabbro zircons may be explained by assimilating high $\delta^{18}O$ older continental crust components into mafic magmas possibly derived from the mantle wedge above subducting oceanic lithosphere.

There are two similar cases reported elsewhere. For instance, high-$\delta^{18}O$(Zrn) values (7.0 to 7.8 ‰) of Cretaceous gabbroic rocks from southern Sierra Nevada Batholith, California, USA, were interpreted to be subduction-related (Lackey et al. 2005). It has been suggested that these mafic magmas may be derived from normal sublithospheric mantle of continental arc type contained in the mantle wedge above subducting oceanic lithosphere, with assimilation of either subducted, hydrothermal altered oceanic crust (Lackey et al. 2005) or continental crust (Nelson et al. 2013). Another example is the Zhengga diorite-gabbro suite from the Gangdese area, southern Tibet, where gabbros have $\delta^{18}O$(Zrn) values of 5.9 to 7.2 ‰ (Ma et al. 2013). These authors conclude that the parental magmas of the Zhengga gabbros were generated by the hydrous partial melting of lithospheric mantle metasomatised by sediment melts/fluids and are therefore also subduction-related. The $\delta^{18}O$ signatures of the meta-gabbro and felsic gneiss from Andros are in accordance with an interpretation suggesting that these rocks are not part of the typical Jurassic ophiolite successions of the Balkan Peninsula but instead formed by partial melting of a metasomatised mantle wedge with significant assimilation of supracrustal material, either hydrothermally altered oceanic crust subducted beneath the volcanic arc or continental crust material. It is noted that the Andros samples have higher radiogenic Nd–Sr isotopic compositions than contemporaneous meta-ophiolites in the region (Bröcker et al. 2014b). However, a more comprehensive dataset would be necessary to robustly constrain this conclusion.

The interpretation for the Late Cretaceous zircons of meta-plagiogranite 4017 is straightforward (Figs. 4, 5). These zircons have $\varepsilon_{Hf}(t)$ values typical for MORB-type mantle, similar to results reported for other Cretaceous zircon populations from Syros and Tinos (Fu et al. 2010, 2012), excluding the group of low-$\delta^{18}O$ zircons with cauliflower-like internal structures and/or porous or dark-CL weakly zoned rims (Fig. 2 of Fu et al. 2012). The average $\delta^{18}O$(Zrn) of 5.5 ± 0.8 ‰ of the pristine grains is also consistent with other mantle-like components (Valley et al. 2005; Cavosie et al. 2009; Grimes et al. 2010).

Such large variations in both $\delta^{18}O$ and $\varepsilon_{Hf}(t)$, especially for older rocks, are not only attributed to complex magmatic processes, but also diverse magma sources. Simple mass balance calculations can be used to assess magma mixing of two endmembers in the region, that is, deeply derived and supracrustal sources (A and B in Fig. 5). The following parameters were used (Fig. 5; see DePaolo 1981): r = (mass of assimilated wallrock into a magma/unit time)/(mass of fractionated crystalline phases effectively separated from the magma/unit time) = 0.6, D = the bulk solid/liquid partition coefficient for the element between the fractionating crystalline phases and the magma = 1, thus $z = (r + D - 1)/(r - 1) = -1.5$. Two endmembers are assumed: Endmember A, $\delta^{18}O = 5.3$ ‰, $\varepsilon_{Hf} = -2$; Endmember B, $\delta^{18}O = 12$ ‰, $\varepsilon_{Hf} = -16$; and $Hf_A/Hf_B = 0.25$. We estimate about 20–30 % by mass supracrustal material was incorporated into mafic magma derived from enriched mantle or lower continental crust during the Late Jurassic. It appears that more and more supracrustal material may be involved in episodic magmatism in the Cyclades over time. Both highest $\delta^{18}O$ values and lowest-$\varepsilon_{Hf}(t)$ values for Triassic to Cenozoic igneous zircons from the Cyclades define an evolution trend consistent with average continental crust, with the exception of Cretaceous zircons formed from depleted MORB mantle sources (Fig. 4).

Tectonic implications

A plausible geodynamic model must account for the following geochemical and isotopic signatures. Combined Pb and Nd isotopic data indicate that the widespread subalkaline basalts of the Hellenides were predominantly derived from previously melt-depleted peridotite within subcontinental lithospheric mantle on the northern margin of Gondwanaland (e.g. Pe-Piper 1998). Unusually high contents of LILE (large ion lithophile elements) in shoshonite and calc-alkaline rocks suggest an additional 'crustal' component that might be associated with a pre-Triassic, possibly Hercynian subduction in heterogenous subcontinental lithosphereic mantle and lower crust (e.g. Pe-Piper 1998; Tsikouras et al. 2008). Triassic rift-related mafic volcanic rocks, abundant in the Hellenides to the west, show enriched mantle and within-plate (rift-related) chemical signatures (E-MORB and OIB: enriched MORB and ocean island basalt) (Bonev et al. 2012).

Taking these aspects into consideration and based on Pe-Piper (1998) and Robertson (2012), we suggest the following scenario for the magmatic evolution of the larger study area (Fig. 6). At ~320 Ma, Paleotethys oceanic crust subducted southwards to the northern margin of Gondwana (e.g. Xypolias et al. 2006), which caused

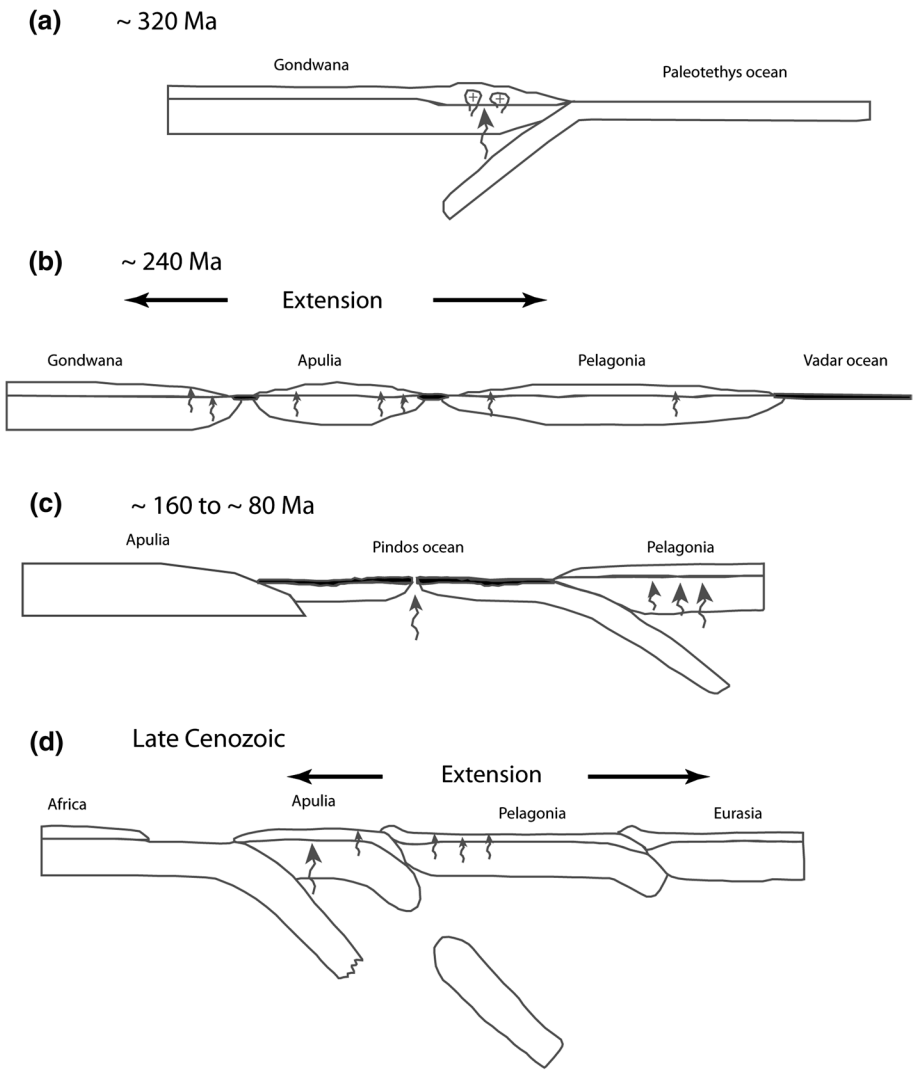

Fig. 6 Tectonic model proposed for the larger Aegean region, modified after Pe-Piper (1998) and Robertson (2012). See text for discussion

partial melting of lower continental crust. At ~240 Ma rift-related magmas were produced from 'enriched' mantle that had been metasomatised by the preceding Hercynian slab melts and/or fluids, and continental crust. The Triassic melts record the separation of the Apulia and (Korabi–) Pelagonia microcontinents from Gondwana. A rift basin further developed and the Pindos (–Mirdita) ocean was formed. At ~160 Ma, Neotethys oceanic lithosphere subducted northwards below Pelagonia and produced Sierra-type gabbros (cf. Lackey et al. 2005). This stage is represented by ~160 Ma meta-gabbros with distinct O–Hf isotopic characteristics. Group B hornblende diorite (hornblende K–Ar age: 154 ± 14 Ma, 2σ) of the calc-alkaline series found as clasts in flysch at Amphissa and characterised by enrichment in REE (rare earch elements) and LILE (Pe-Piper and Koukouvelas 1992) might be another example of Jurassic gabbroic rocks of the same type. At ~80 Ma, MORB formed at spreading centres of small Neotethys ocean basins. The remnant Pindos oceanic crust subducted and closed progressively southwards during Cretaceous and Tertiary times. During the Late Cenozoic, orogeny I and S-type granites were formed (Bolhar et al. 2010, 2012).

Conclusions

Zircon U–Pb, O, and Hf isotopic data of meta-igneous rocks representing mélanges and marble–schist sequences from the islands of Andros, Ios, Sifnos, and Syros were used to define the crustal evolution of the Attic–Cycladic Crystalline Belt. The following conclusions can be reached:

1. Middle Triassic igneous zircons characterised by variable $\delta^{18}O$ and $\varepsilon_{Hf}(t)$ values could have formed from different sources, that is, metasomatised mantle and lower continental crust. The results of this study are in accordance with the interpretation that Triassic mag-

matism in the Hellenides is not subduction- but more likely rift-related (e.g. Pe-Piper 1998).

2. Late Jurassic igneous zircons of a meta-gabbro from Andros have higher $\delta^{18}O$ but lower $\varepsilon_{Hf}(t)$ values than zircons from an associated felsic gneiss with the same protolith age, arguing against MORB affinity. This supports the conclusion that the Jurassic gabbroic rocks from Andros do not belong to the group of SSZ-type ophiolites that are widespread along the margin of the Pelagonian zone (Pe-Piper and Koukouvelas 1992), but represent a distinct group recording partial melting of metasomatised mantle wedge with significant assimilation of supracrustal material.
3. Late Cretaceous igneous zircons are characterised by MORB-like $\delta^{18}O$ and $\varepsilon_{Hf}(t)$ values, suggesting that the Late Cretaceous magmas were produced by partial melting of depleted MORB mantle (see also Fu et al. 2010, 2012).
4. The Mesozoic magmatic rocks of the Attic–Cycladic Crystalline Belt record reworking of older continental crust with input of multiple mantle components or juvenile components over certain periods of time.

Acknowledgments Sue Keay kindly provided an electronic copy of her PhD dissertation. The authors thank Georgia Pe-Piper and Petek Ayda Ustaömer for their constructive comments on an earlier version of this manuscript, and Wolf-Christian Dullo for his editorial handling.

References

Avigad D (1993) Tectonic juxtaposition of blueschists and greenschists in Sifnos Island (Aegean Sea): implications for the structure of the Cycladic blueschist belt. J Struct Geol 15:1459–1469

Avigad D, Matthews A, Evans BW, Garfunkel Z (1992) Cooling during exhumation of a blueschist terrane: Sifnos (Cyclades, Greece). Eur J Mineral 4:619–634

Baldwin SL, Lister GS (1998) Thermochronology of the South Cyclades Shear Zone, los, Greece: effects of ductile shear in the argon partial retention zone. J Geophys Res (Solid Earth) 103:7315–7336

Bindeman IN, Eiler JM, Yogodzinski GM, Tatsumi Y, Stern CR, Grove TL, Portnyagin M, Hoernle K, Danyushevsky LV (2005) Oxygen isotope evidence for slab melting in modern and ancient subduction zones. Earth Planet Sci Lett 235:480–496

Bolhar R, Ring U, Allen CM (2010) An integrated zircon geochronological and geochemical investigation into the Miocene plutonic evolution of the Cyclades, Aegean Sea, Greece: part 1: geochronology. Contrib Mineral Petrol 160:719–742

Bolhar R, Ring U, Kemp AIS, Whitehouse MJ, Weaver SD, Woodhead JD, Uysal IT, Turnbull R (2012) An integrated zircon geochronological and geochemical investigation into the Miocene plutonic evolution of the Cyclades, Aegean Sea, Greece: part 2: geochemistry. Contrib Mineral Petrol 164:915–933

Bonev N, Dilek Y, Hanchar JM, Bogdanov K, Klain L (2012) Nd–Sr–Pb isotopic composition and mantle sources of Triassic rift units in the Serbo-Macedonian and the western Rhodope massifs (Bulgaria–Greece). Geol Mag 149:146–152

Bortolotti V, Chiari M, Marroni M, Pandolfi L, Principi G, Saccani E (2013) Geodynamic evolution of ophiolites from Albania and Greece (Dinaric-Hellenic belt): one, two, or more oceanic basins? Int J Earth Sci (Geol Rundsch) 102:783–811

Bröcker M, Franz L (1998) Rb–Sr isotope studies on Tinos Island (Cyclades, Greece): additional time constraints for metamorphism, extent of infiltration-controlled overprinting and deformational activity. Geol Mag 135:369–382

Bröcker M, Franz L (2006) Dating metamorphism and tectonic juxtaposition on Andros Island (Cyclades, Greece): results of a Rb–Sr study. Geol Mag 143:609–620

Bröcker M, Keasling A (2006) Ion probe U–Pb zircon ages from the high-pressure/low-temperature mélange of Syros, Greece: age diversity and the importance of pre-Eocene subduction. J Metamorp Geol 24:615–631

Bröcker M, Pidgeon RT (2007) Protolith ages of meta-igneous and metatuffaceous rocks from the Cycladic Blueschist Unit, Greece: results of a reconnaissance U–Pb zircon study. J Geol 115:83–98

Bröcker M, Huyskens M, Berndt J (2014a) U–Pb dating of detrital zircons from Andros, Greece: constraints for the time of sediment accumulation in the northern part of the Cycladic blueschist belt. Geol J, submitted

Bröcker M, Löwen K, Rodionov N (2014b) Unraveling protolith ages of meta-gabbros from Samos and the Attic–Cycladic Crystalline Belt, Greece: results of a U–Pb zircon and Sr–Nd whole rock study. Lithos 198–199:234–248

Bulle F, Bröcker M, Gärtner C, Keasling A (2010) Geochemistry and geochronology of HP mélanges from Tinos and Andros, cycladic blueschist belt, Greece. Lithos 117:61–81

Cavosie AJ, Kita NT, Valley JW (2009) Magmatic zircons from the Mid-Atlantic Ridge: primitive oxygen isotope signature. Am Mineral 94:926–934

Chatzaras V, Dörr W, Finger F, Xypolias P, Zulauf G (2013) U-Pb single zircon ages and geochemistry of metagranitoid rocks in the Cycladic Blueschists (Evia Island): implications for the Triassic tectonic setting of Greece. Tectonophysics 595–596:125–139

DePaolo DJ (1981) Trace element and isotopic effects of combined wallrock assimilation and fractional crystallisation. Earth Planet Sci Lett 53:189–202

Dixon JE, Ridley JR (1987) Syros. In: Helgeson HC (ed) Chemical transport in metasomatic processes. Reidel Publishing Company, Dordrecht, pp 489–501

Dürr S, Altherr R, Keller J, Okrusch M, Seidel E (1978) The Median Aegean Crystalline Belt: stratigraphy, structure, metamorphism, magmatism. In: Closs H, Roeder DH, Schmidt K (eds) Alps, Apennines, Hellenides. IUGS report no. 38, Schweizerbart, Stuttgart, pp 455–477

Eggins SM, Grün R, McCulloch MT, Pike AWG, Chappell J, Kinsley L, Mortimer G, Shelley M, Murray-Wallace CV, Spötle C, Taylor L (2005) In situ U-series dating by laser-ablation multi-collector ICPMS: new prospects for Quaternary geochronology. Quat Sci Rev 24:2523–2538

Eiler JM (2001) Oxygen isotope variations of basaltic lavas and upper mantle rocks. In: Valley JW, Cole DR (eds) Stable isotope geochemistry. Rev Mineral Geochem 43:319–364. Mineralogical Society of America/Geochemical Society, Washington, DC

Forster MA, Lister GS (1999) Detachment faults in the Aegean core complex of Ios, Cyclades, Greece. Geol Soc Lond Spec Publ 154:305–323

Fu B, Valley JW, Kita NT, Spicuzza MJ, Paton C, Tsujimori T, Bröcker M, Harlow GE (2010) Multiple origins of zircons in jadeitite. Contrib Mineral Petrol 159:769–780

Fu B, Paul B, Cliff J, Bröcker M, Bulle F (2012) O-Hf isotope constraints on the origin of zircons in high-pressure mélange blocks and associated matrix rocks from Tinos and Syros, Greece. Eur J Mineral 24:277–287

Geldmacher J, Hoernle K, Hanan BB, Blichert-Toft J, Hauff F, Gill JB, Schmincke HU (2011) Hafnium isotopic variations in East Atlantic intraplate volcanism. Contrib Mineral Petrol 162:21–36

Grimes CB, Ushikubo T, John BE, Valley JW (2010) Uniformly mantle-like $\delta^{18}O$ in zircons from oceanic plagiogranites and gabbros. Contrib Mineral Petrol 161:13–33

Groppo C, Forster M, Lister G, Compagnoni R (2009) Glaucophane schists and associated rocks from Sifnos (Cyclades, Greece): new constraints on the P–T evolution from oxidized systems. Lithos 109:254–273

Hawkesworth CJ, Kemmp AIS (2006) Using hafnium and oxygen isotopes in zircons to unravel the record of crustal evolution. Chem Geol 226:144–162

Henjes-Kunst F, Kreuzer H (1982) Isotopic dating of pre-Alpidic rocks from the island of Ios (Cyclades, Greece). Contrib Mineral Petrol 80:245–253

Himmerkus F, Reischmann T, Kostopoulos D (2009) Triassic rift-related meta-granites in the Internal Hellenides, Greece. Geol Mag 146:252–265

Huet B, Labrousse L, Jolivet L (2009) Thrust or detachment? Exhumation processes in the Aegean: insight from a field study on Ios (Cyclades, Greece). Tectonics 28, TC3007. doi:10.1029/2008TC002397

Huyskens MH, Bröcker M (2014) The status of the Makrotantalon Unit (Andros, Greece) within the structural framework of the Attic–Cycladic Crystalline Belt. Geol Mag 151:430–446

Ickert RB, Hiess J, Williams IS, Holden P, Ireland TR, Lanc P, Schram N, Foster JJ, Clement SW (2008) Determining high precision, in situ, oxygen isotope ratios with a SHRIMP II: analyses of MPI-DING silicate-glass reference materials and zircon from contrasting granites. Chem Geol 257:114–128

Ireland TR, Williams IS (2003) Considerations in zircon geochronology by SIMS. In: Hanchar JM, Hoskin PWO (eds) Zircon. Rev Mineral Geochem 53:215–241. Mineralogical Society of America/Geochemical Society, Washington, DC

Ji WQ, Wu FY, Chung SL, Li JX, Liu CZ (2009) Zircon U–Pb geochronology and Hf isotopic constraints on petrogenesis of the Gangdese batholith, southern Tibet. Chem Geol 262:229–245

Keay S (1998) The Geological Evolution of the Cyclades, Greece: Constraints from SHRIMP U–Pb Geochronology. Unpubl PhD Dissertation, Australian National University, Canberra, pp 341

Keay S, Lister G (2002) African provenance for the metasediments and metaigneous rocks of the Cyclades, Aegean Sea, Greece. Geology 30:235–238

Keiter M, Ballhaus C, Tomaschek F (2011) A New Geological Map of the Island of Syros (Aegean Sea, Greece): implications for Lithostratigraphy and Structural History of the Cycladic Blueschist Unit. Geol Soc Am Spec Paper 481:1–43

Koutsovitis P, Magganas A, Ntaflos T (2012) Rift and intra-oceanic subduction signatures in the Western Tethys during the Triassic: the case of ultramafic lavas as part of an unusual ultramafic–mafic–felsic suite in Othris, Greece. Lithos 144–145:177–193

Lackey JS, Valley JW, Saleeby JB (2005) Supracrustal input to magmas in the deep crust of Sierra Nevada batholith: evidence from high-$\delta^{18}O$ zircon. Earth Planet Sci Lett 235:315–330

Löwen K, Bröcker M, Berndt J (2014) Depositional ages of clastic metasediments from Samos and Syros, Greece: results of a detrital zircon study. Int J Earth Sci (Geol Rundsch). doi:10.1007/s00531-014-1058-x (in press)

Ludwig KR (2001a) User's Manual for Isoplot/Ex rev. 2.49: a geochronological toolkit for Microsoft Excel. Berkeley Geochronological Center Special Publication no. 1a

Ludwig KR (2001b) SQUID 1.02, A user's manual. Berkeley Geochronological Center Special Publication no. 2

Ma L, Wang Q, Wyman DA, Jiang ZQ, Yang JH, Li QL, Gou GN, Guo HF (2013) Late Cretaceous crustal growth in the Gangdese area, southern Tibet: petrological and Sr–Nd–Hf–O isotopic evidence from Zhengga diorite–gabbro. Chem Geol 349–350:54–70

Martin E, Bindeman I, Grove TL (2011) The origin of high-Mg magmas in Mt Shasta and Medicine Lake volcanoes, Cascade Arc (California): higher and lower than mantle oxygen isotope signatures attributed to current and past subduction. Contrib Mineral Petrol 162:945–960

Meinhold G, Reischmann T, Kostopoulos D, Lehnert O, Matukov D, Sergeev S (2008) Provenance of sediments during subduction of Palaeotethys: detrital zircon ages and olistolith analysis in Palaeozoic sediments from Chios Island, Greece. Palaeogeogr Palaeoclimatol Palaeoecol 263:71–91

Mukhin P (1996) The metamorphosed olistostromes and turbidites of Andros Island, Greece, and their tectonic significance. Geol Mag 133:697–711

Murphy JB, Nance RD, Cawood PA (2009) Contrasting modes of supercontinent formation and the conundrum of Pangea. Gondwana Res 15:408–420

Nelson WR, Dorais MJ, Christiansen EH, Hart GL (2013) Petrogenesis of Sierra Nevada plutons inferred from the Sr, Nd, and O isotopic signatures of mafic igneous complexes in Yosemite Valley, California. Contrib Mineral Petrol 165:397–417

Nowell GM, Kempton PD, Noble SR, Fitton JG, Saunders AD, Mahoney JJ, Taylor RN (1998) High precision Hf isotope measurements of MORB and OIB by thermal ionisation mass spectrometry: insights into the depleted mantle. Chem Geol 149:211–223

Okrusch M, Bröcker M (1990) Eclogite facies rocks in the Cycladic blueschist belt, Greece: a review. Eur J Mineral 2:451–478

Papanikolaou D (1978) Contribution to the geology of the Aegean Sea: the island of Andros. Ann Géol Pays Hellén 29:477–553

Paton C, Hellstrom J, Paul B, Woodhead J, Hergt J (2011) Iolite: freeware for the visualisation and processing of mass spectrometric data. J Anal At Spectrom 26:2508–2518

Patzak M, Okrusch M, Kreuzer H (1994) The Akrotiri unit on the island of Tinos, Cyclades, Greece: witness to a lost terrane of Late Cretaceous age. Neues Jahrb Geol Palaontol Abh 194:211–252

Pe-Piper G (1998) The nature of Triassic extension-related magmatism in Greece: evidence from Nd and Pb isotope geochemistry. Geol Mag 135:331–348

Pe-Piper G, Koukouvelas I (1992) Petrology, geochemistry and regional geological significance of igneous clasts in Parnassus flysch, Amphissa area, Greece. Neues Jahrb Mineral Abh 164:94–112

Pe-Piper G, Piper DJW (2002) The igneous rocks of Greece: the anatomy of an orogen. Borntraeger, Berlin, p 573

Perkins GB, Sharp ZD, Selverstone J (2006) Oxygen isotope evidence for subduction and rift-related mantle metasomatism beneath the Colorado Plateau–Rio Grande rift transition. Contrib Mineral Petrol 151:633–650

Pfänder JA, Münker C, Stracke A, Mezger K (2007) Nb/Ta and Zr/Hf in ocean island basalts—implications for crust–mantle differentiation and the fate of Niobium. Earth Planet Sci Lett 254:158–172

Reischmann T (1998) Pre-Alpine origin of tectonic units from the metamorphic complex of Naxos, Greece, identified by single zircon Pb/Pb dating. Bull Geol Soc Greece 22:101–111

Ring U, Glodny J, Will T, Thomson S (2010) The Hellenic subduction system: high-pressure metamorphism, exhumation, normal faulting, and large-scale extension. Ann Rev Earth Planet Sci 38:45–76

Roberts NMW, Slagstad T, Parrish RR, Norry MJ, Marker M, Horstwood MSA (2013) Sedimentary recycling in arc magmas: geochemical and U–Pb–Hf–O constraints on the Mesoproterozoic Suldal Arc, SW Norway. Contrib Mineral Petrol 165:507–523

Robertson AHF (2012) Late Palaeozoic–Cenozoic tectonic development of Greece and Albania in the context of alternative

reconstructions of Tethys in the Eastern Mediterranean region. Int Geol Rev 54:373–454

Robertson AHF, Clift PD, Degnan PJ, Jones G (1991) Palaeogeographic and palaeotectonic evolution of the Eastern Mediterranean Neotethys. Palaeogeogr Palaeoclimatol Palaeoecol 87:289–343

Schliestedt M (1986) Eclogite-blueschist relationships as evidenced by mineral equilibria in the high-pressure metabasic rocks of Sifnos (Cycladic Islands), Greece. J Petrol 27:1437–1459

Schliestedt M, Matthews A (1987) Transformation of blueschist to greenschist facies rocks as a consequence of fluid infiltration, Sifnos (Cyclades) Greece. Contrib Mineral Petrol 97:237–250

Schmädicke E, Will TM (2003) Pressure-temperature evolution of blueschist facies rocks from Sifnos, Greece, and implications for the exhumation of high-pressure rocks in the Central Aegean. J Metamorph Geol 21:799–811

Schumacher J, Brady JB, Cheney JT, Tonnsen RR (2008) Glaucophane-bearing Marbles on Syros, Greece. J Petrol 49:1667–1686

Thomson SN, Ring U, Brichau S, Glodny J, Will TM (2009) Timing and nature of formation of the ios metamorphic core complex, southern Cyclades, Greece. Geol Soc Lond Spec Publ 321:139–167

Trotet F, Vidal O, Jolivet L (2001a) Exhumation of Syros and Sifnos metamorphic rocks (Cyclades, Greece): new constraints on the P–T paths. Eur J Mineral 13:901–920

Trotet F, Jolivet L, Vidal O (2001b) Tectono-metamorphic evolution of Syros and Sifnos (Cyclades, Greece). Tectonophysics 338:179–206

Tsikouras B, Pe-Piper G, Piper DJ, Hatzipanagiotou K (2008) Triassic rift-related komatiite, picrite and basalt, Pelagonian continental margin, Greece. Lithos 104:199–215

Valley JW, Lackey JS, Cavosie AJ, Clechenko CC, Spicuzza MJ, Basei MAS, Bindeman IN, Ferreira VP, Sial AN, King EM, Peck WH, Sinha AK, Wei CS (2005) 4.4 billion years of crustal maturation: oxygen isotopes in magmatic zircon. Contrib Mineral Petrol 150:561–580

van der Maar PA, Jansen JBH (1983) The geology of the polymetamorphic complex of Ios, Cyclades, Greece and its significance for the Cycladic massif. Geol Rundsch 72:283–299

von Raumer JF (1998) The Palaeozoic evolution in the Alps: from Gondwana to Pangea. Geol Rundsch 87:407–435

Williams IS (1998) U–Th–Pb geochronology by ion microprobe. In: McKibben MA, Shanks III WC, Ridely WI (eds) Applications of microanalytical techniques to understanding mineralizing processes. Rev Econ Geol 7:1–35

Woodhead JD, Hergt JM, Davidson JP, Eggins SM (2001) Hafnium isotope evidence for 'conservative' element mobility during subduction zone processes. Earth Planet Sci Lett 192:331–346

Xypolias P, Dörr W, Zulauf G (2006) Late Carboniferous plutonism within the pre-Alpine basement of the External Hellenides (Kithira, Greece): evidence from U–Pb zircon dating. J Geol Soc London 163:539–547